# HUMAN FACTORS IN FUNDAMENTAL DIAGRAM

Daiheng Ni
Department of Civil and Environmental Engineering
University of Massachusetts Amherst
130 Natural Resources Road, Amherst, MA 01003
Phone: (413) 545-5408
Email: ni@ecs.umass.edu

Linbo Li
Department of Traffic Engineering
Tongji University
4800 Cao An Highway, Shanghai, China 201804
Phone: (021) 6958-3007
Email: llinbo@tongji.edu.cn

Haizhong Wang
Department of Civil and Construction Engineering
Oregon State University
Phone: (541) 737- 8538
Email: Haizhong.Wang@oregonstate.edu

Chaoqun (Enzo) Jia
Department of Civil and Environmental Engineering
University of Massachusetts Amherst
130 Natural Resources Road, Amherst, MA 01003
Email: cjia@umass.edu

**Abstract**

Some observations are made on fundamental diagram of freeway traffic, among which are three influence regions, three types of transition around capacity, and capacity drop phenomenon. This research aspires to interpret these observations from a human factors perspective in traffic flow theory. Of particular interest are the following human factors: drivers' choice of desired speeds, perceived effective vehicle lengths, perception-reaction times, and aggressiveness. It appears that all four factors are involved in characterizing traffic flow, though they play different roles in the fundamental diagram. Different combinations of these factors give rise to the above-mentioned influence regions, transition around capacity, and capacity drop. Of critical importance in determining the transition around capacity and capacity drop is drivers' aggressiveness – a factor that has long been overlook in the past. This paper provides a detailed account of where it comes from and how it influences the fundamental diagram.

## SOME FIELD OBSERVATIONS

Figure 1 illustrates an empirical fundamental diagram observed on Georgia 400, a toll road in Atlanta, GA. Each point in the "cloud" represents a 5-minute aggregation of the original 20-second observations and the diagram consists of one year worth of data.

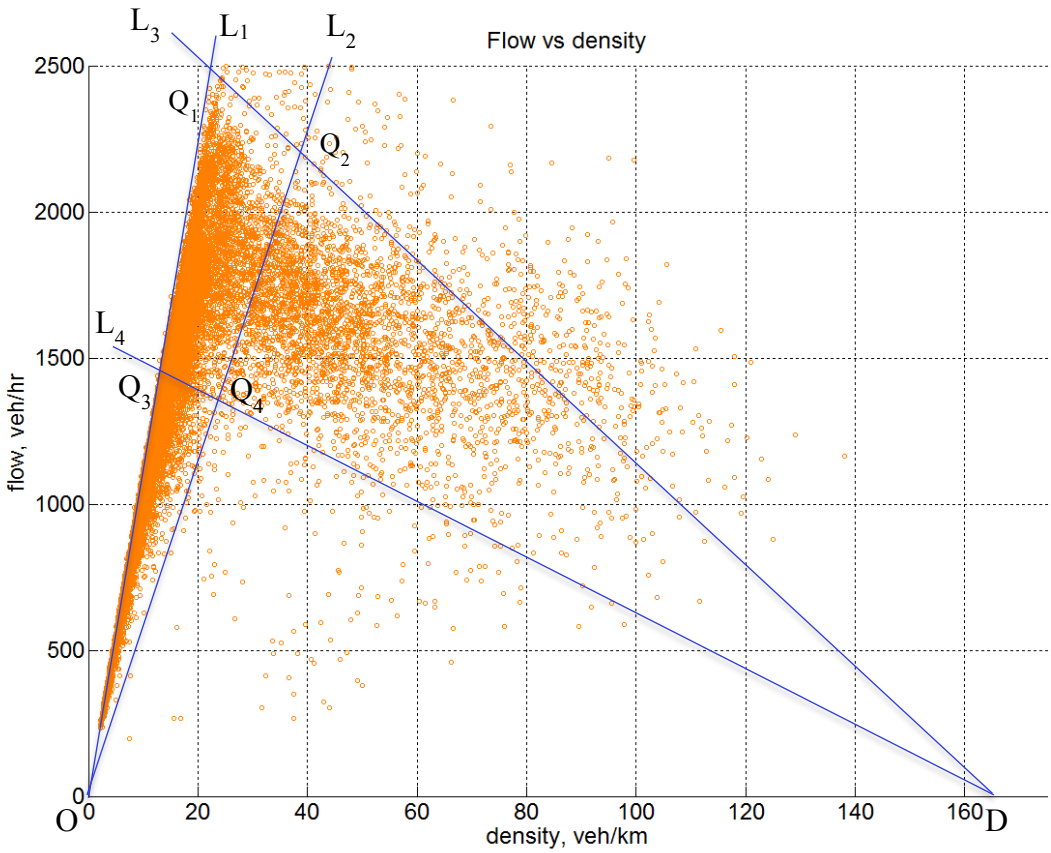


**FIGURE 1 Fundamental diagram resulted from field observations.**

### Observation 1 – Three Influence Regions

Strikingly in this diagram are the following regions. One is the area bounded by lines $L_1$ and $L_2$ just like a beam of light emitting from the origin O; the other is the area bounded by lines $L_3$ and $L_4$ like another beam of light emitting from point D which represents jam density $k_j$. The area $Q_1Q_2Q_3Q_4$ indicates a third region where the two beams of light interfere.

Obviously, area $L_1OL_2$ indicates free-flow conditions where flow is dictated by free-flow speed, area $L_3DL_4$ consists of congested conditions where flow is mainly constrained by drivers' perception-reaction capabilities. Influenced by both free-flow and congested regions, area $Q_1Q_2Q_3Q_4$ constitutes a *capacity region* since this is where the capacity is most likely to be found.

It is intriguing to explore what factors are acting behind that drive the shaping of the diagram. Of key interests here are capacity condition (magnitude and location), the transition of flow-density relationship around capacity, and whether or not there is capacity drop phenomenon.

**Observation 2 – Three Types of Transition in Flow-Density Relationship**

Observed in the field are the following three types of transition regarding flow-density relationship around capacity:

- Skewed-parabola, e.g., curve 1 in Figure 2 below,
- Triangular, e.g., curve 2 in Figure 2, and
- Reverse-lambda, e.g., curve 3 in Figure2,

where a reverse-lambda transition is most likely found in inner lane traffic, a triangular transition is often resulted in middle lane traffic or by aggregating over all lanes, and a skewed-parabola transition is typical in outer lane traffic. These empirical observations have been reported by Koshi et al [1], Banks [2], and others.

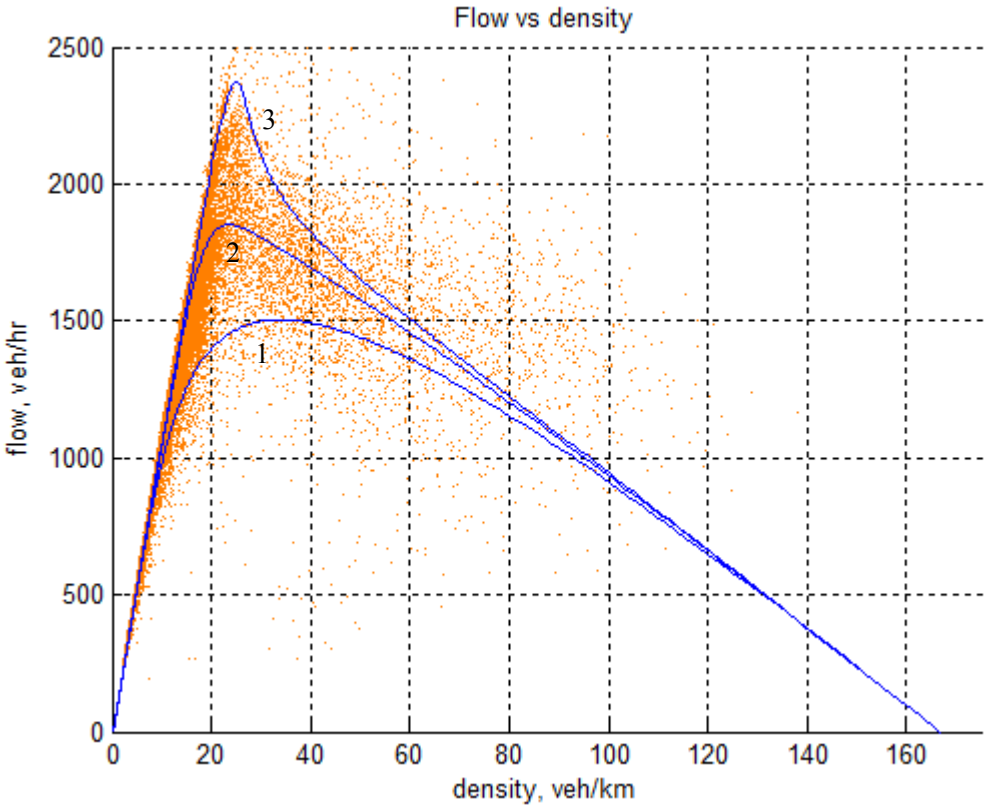


**FIGURE 2 Flow-density relationships fitted to empirical data.**

We have models that capture the skewed-parabola flow-density relationship as well as a few other models that represent the triangular flow-density relationship. It is of great interest to understand what gives rise to these types of flow-density relationships. In particular, what causes the reverse-lambda transition and how to model it?

## Observation 3 – Capacity drop

Figure 3 is another fundamental diagram generated from GA400, but this figure only includes one day worth of data on a week day, see the "cloud" in the background. Consisting of observations of flow and density in the field, each data point represents the operating condition of traffic over this observation period. A time development of operating conditions is plotted on top of the "cloud" with numbers indicating the temporal order of the observations of roughly 10 minutes apart. Note that the peak flow occurs at around 7:30am which is numbered 14 in the figure.

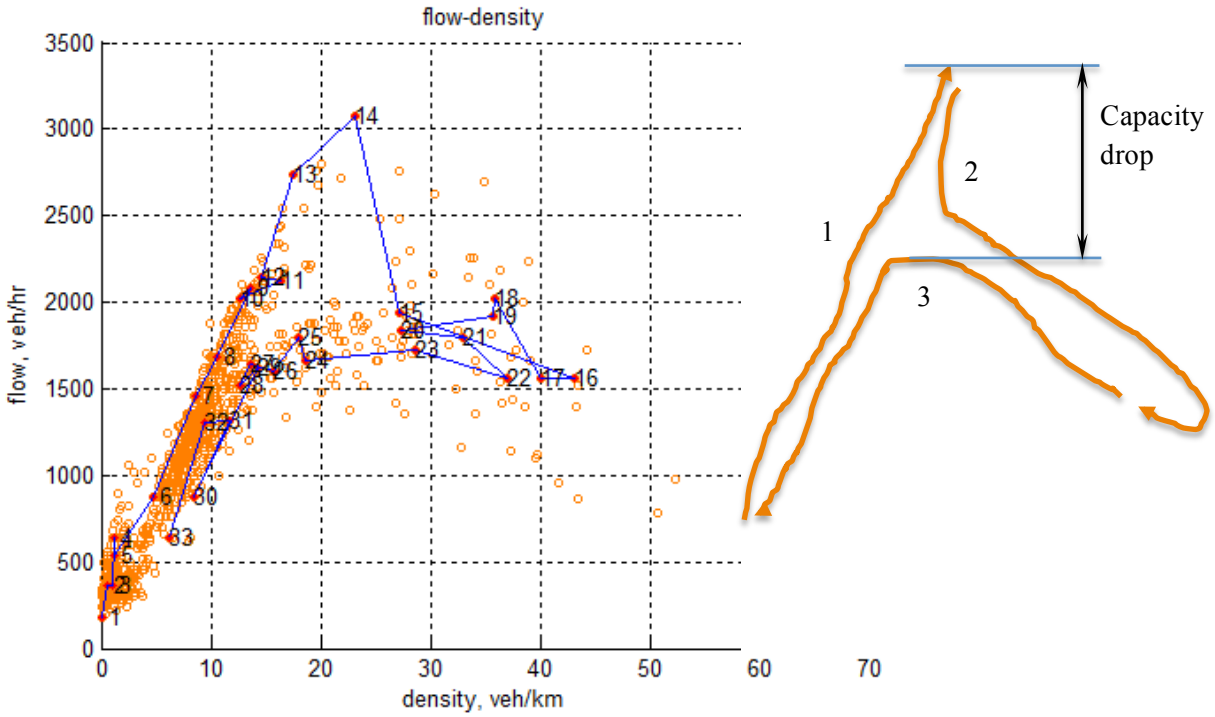


**FIGURE 3 Time series plot of loading and unloading process**

Following the time development, the temporal evolution of traffic conditions around capacity seems to suggest a pattern sketched on the right of the figure. First, there is a loading process early in the morning as the road starts empty and traffic demand increases over time. This is sketched as curve 1 in the figure where flow increases almost linearly with density all the way up to the peak. As demand continues increasing beyond the peak, any disturbance may result in traffic breakdown and hence congestion. This corresponds to curve 2 in the figure. As demand decreases, traffic begins to unload where density decreases and flow increases as in the first half of curve 3. However, the peak of the unloading curve is much less than that of the loading curve and their difference constitutes a *capacity drop* phenomenon. With demand continue decreasing, both flow and density drop, as depicted in the second half of curve 3. This concludes a cycle of traffic operation in a typical day. Similar findings of traffic loading, unloading, and capacity drop have been reported in [3] [4] [5]. Interested readers are motivated to investigate whether it is possible to capture such a phenomenon in traffic flow modelling.

With these observations and questions, the objective of this paper is to explore factors acting behind a fundamental diagram that give rise to these phenomena. The remainder of the paper is organized as follows. First, we start with examining human factors in car following and trace their way into macroscopic representation of traffic flow – the fundamental diagram. Next, we analyze the roles that these human factors play in fundamental diagram, in particular, which factor controls what part of the diagram? This is followed by a revisit to empirical data and check if field observations agree with the above analysis. To facilitate application of findings of this research, a method is formulated to roughly estimate human factors parameters from traffic flow data without requiring vehicle trajectory data. Lastly, findings are summarized and conclusions are drawn.

## RELATING HUMAN FACTORS TO FUNDAMENTAL DIAGRAM

In essence, traffic flow is the result of action and interaction of many vehicles in a driving environment. The microscopic view of traffic flow is the result of human factors such as drivers' speed choice, perception-reaction time, acceleration and deceleration, and safety rules. On the other hand, the macroscopic view of traffic flow is typically reflected in a fundamental diagram that is characterized by macroscopic measures such as capacity, free-flow speed, and jam density. Micro-macro coupling is the key to unlock fundamental diagram. In this paper, we are particularly interested in how human factors are related to highway capacity and traffic congestion and, in return, how the discovery would shed light on traffic flow modelling.

### Microscopic View – Human Factors

*Stopping Sight Distance*

Traffic engineering books [6] [7] [8] have it as a standard that safe stopping sight distance ($SSD$) has to be maintained at any point on a roadway. The $SSD$ is the sum of distance traveled during perception-reaction time $\tau$ and braking distance:

$$SSD = \tau v + \frac{v^2}{2b}$$

where $v$ is vehicle speed and $b$ is deceleration rate.

*Good Driving Rule (GDR)*

Similarly, Forbes [9] and equivalently Pipes [10] applied a "good driving rule" to car following and stipulated that the minimum spacing $s^*$ between a leading vehicle $j$ and a following vehicle $i$ be:

$$s_{ij}^* = \tau_i \dot{x}_i + l_j$$

where $l$ is effective vehicle length, i.e. actual vehicle length plus some buffer space at both ends.

*Safe Driving Rule (SDR)*

Gipps [11] took it further by considering more dynamic and conservative situations between vehicles with speeds $\dot{x}_i$ and $\dot{x}_j$ and deceleration rates $b_i$ and $B_j$ as follows. At any time, vehicle $i$ must leave enough spacing ahead such that, when vehicle $j$ suddenly brakes, the spacing should allow vehicle $i$ to stop safely behind vehicle $j$ after a perception-reaction process and a braking process. A simplified expression of this "safe driving rule" can be formulated as:

$$s_{ij}^* = \frac{\dot{x}_i^2}{2b_i} - \frac{\dot{x}_j^2}{2B_j} + \tau_i \dot{x}_i + l_j$$

If the vehicles travel at the same speed, i.e., $\dot{x}_i = \dot{x}_j$, the above equation reduces to the following form [12] [13] (Chapter 4):

$$s_{ij}^* = \gamma_i \dot{x}_i^2 + \tau_i \dot{x}_i + l_j$$

where the coefficient of the non-linear term $\gamma_i$ is

$$\gamma_i = \frac{1}{2}\left(\frac{1}{b_i} - \frac{1}{B_j}\right)$$

Unlike perception-reaction time $\tau$, the physical meaning of $\gamma$ was not defined, but the coefficient was generally regarded as positive. An empirical value for $\gamma$ would be 0.023 $s^2$/ft (about 0.075 $s^2$/m) [12].

*Aggressive Driving Rule (ADR)*

A less conservative consideration of $\gamma_i$ [14] may be resulted by choosing proper values for $b_i$ and $B_j$. For example, it is recognized that $b_i$ actually represents the deceleration rate at which driver $i$ believes that he or she is capable of applying in an emergency. Of particular interest is the possibility that $b_i$ might be greater in magnitude than $B_j$ which represents driver $i$'s estimate of the emergency deceleration that is most likely to be applied by driver $j$. Consequently, $\gamma_i$ may take negative values: $\gamma_i < 0$, which gives rise to an "aggressive driving rule". Rather than creating an extra safety buffer as in the safe driving rule, the negative driving rule even shorten the safe distance stipulated by the good driving rule.

In sum, when $\gamma_i = 0$ as in Forbes model, the good driving rule is resulted; when $\gamma_i > 0$ as in Gipps model, the safe driving rule is resulted since the driver leaves extra room; when $\gamma_i < 0$, the aggressive driving rule is resulted in that the driver tends to follow dangerously close. Hence, it is reasonable to associate $\gamma_i$ to the driver's *aggressiveness* since it represents the driver's willingness to run risk in trade of speed gain.

*Longitudinal Control Model (LCM)*

The aggressive driving rule alone was not modeled. However, Ni [15] recently incorporated the concept of aggressiveness into Longitudinal Control Model (LCM):

$$\ddot{x}_i(t+\tau_i) = A_i\left[1 - \left(\frac{\dot{x}_i}{v_i}\right) - e^{1-\frac{s_{ij}}{s_{ij}^*}}\right]$$

where $v_i$ is driver $i$'s desired speed and $A_i$ is the maximum acceleration desired by driver $i$ when starting from standing still. Note that $s_{ij}^* = \gamma_i \dot{x}_i^2 + \tau_i \dot{x}_i + l_j$ and aggressiveness $\gamma_i$ is allowed to be positive, zero, and negative representing a spectrum of driving rules.

The discussion on traffic flow models thus far has involved a few human factors parameters including aggressiveness $\gamma_i$, perception-reaction time $\tau_i$, desired speed $v_i$, and effective vehicle length $l_i$. It is interesting to examine how these parameters manifest themselves in the fundamental diagram where individual behaviors are aggregated to exhibit collective properties of traffic flow.

**Macroscopic View – the Fundamental Diagram**

Characterizing the fundamental diagram are flow-speed-density relationships. Under steady-state condition, i.e., traffic state does not change in time, the good driving rule gives rise to the following flow $q$ and density $k$ relationship:

$$q = \frac{1}{\tau} - \frac{l}{\tau}k$$

where $\tau$ and $l$ are perception-reaction time $\tau_i$ and effective vehicle length $l_j$, respectively, aggregated over all vehicles. Similarly, the flow-density relationship implied by the safe driving rule is given in parametric form:

$$q = kv \quad \text{and} \quad k = \frac{1}{\gamma v^2 + \tau v + l}$$

where $\gamma$ and $l$ are $\gamma_j$ and $l_j$, respectively, aggregated over all vehicles. The parametric flow-density relationship of LCM is

$$q = kv \quad \text{and} \quad k = \frac{1}{(\gamma v^2 + \tau v + l)[1 - \ln\left(1 - \frac{v}{v_f}\right)]}$$

where free-flow speed $v_f$ is desired speed $v_i$ aggregated over all vehicles.

**INFLUENCE OF HUMAN FACTORS ON FUNDAMENTAL DIAGRAM**

**Desired Speed $v_i$**

The foremost of the set of human factors parameters is desired speed $v_i$. When traffic is light and actual spacing $s_{ij}$ is greater than desired spacing $s_{ij}^*$, drivers are insensitive to neighboring vehicles and are free to choose their desired speed $v_i$. This is what safe driving rule, good driving rule, and LCM stipulate, i.e.,

SDR: $\dot{x}_i = v_i$ when $s_{ij} > s_{ij}^* = \gamma_i \dot{x}_i^2 + \tau_i \dot{x}_i + l_j$
GDR: $\dot{x}_i = v_i$ when $s_{ij} > s_{ij}^* = \quad \tau_i \dot{x}_i + l_j$
LCM: $\dot{x}_i = v_i \left(1 - e^{1 - \frac{s_{ij}}{s_{ij}^*}}\right)$ for all $s_{ij}$ where $\dot{x}_i \sim v_i$ when $s_{ij} > s_{ij}^*$.

When aggregated over drivers, desired speed becomes free-flow speed: $v_i \to v_f$. Therefore, all three models agree that desired speed dictates free-flow speed which, in turn, determines traffic conditions in the free-flow region of Figure 1. As Forbes [16] pointed out, flow $q$ increases linearly with density $k$ without being constrained by leading vehicles. This effect is illustrated in the top left subplot of Figure 4 which is generated using LCM. In this plot, free-flow speed varies while other three parameters are held constant as indicated. Units are in metric system.

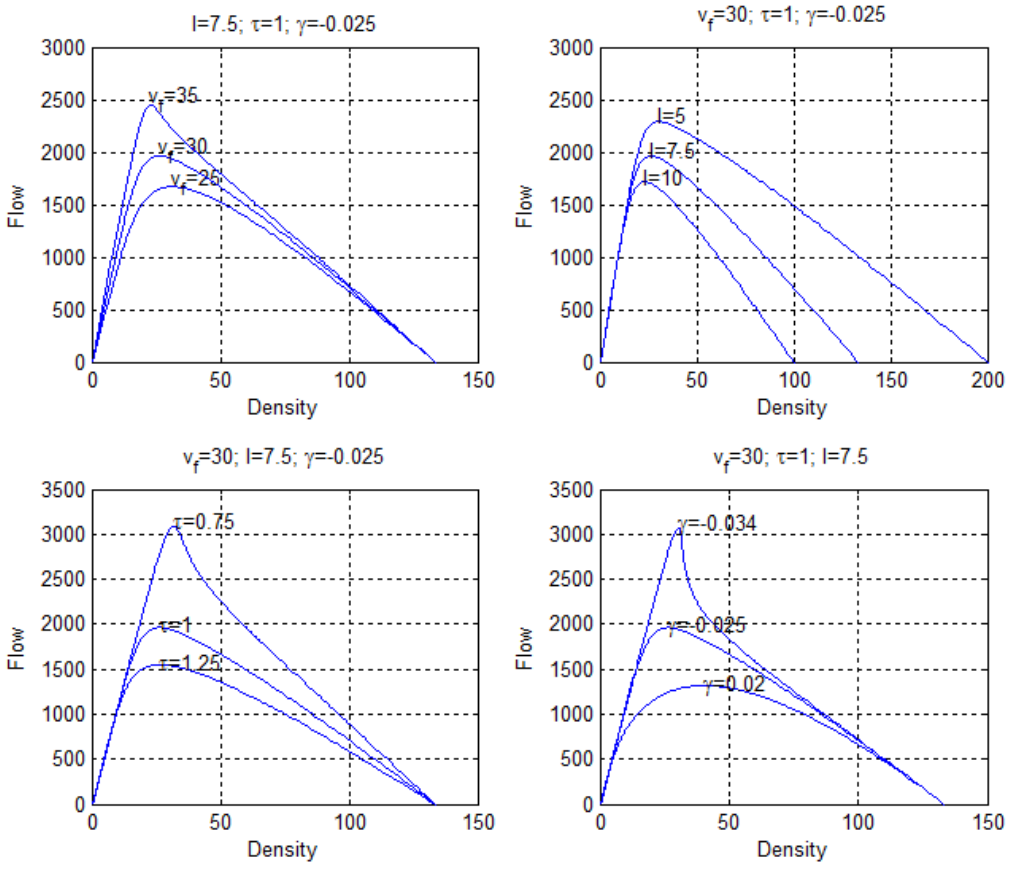


**FIGURE 4 Influence of human factors on fundamental diagram**

The capacity condition of SDR is found at:

$$q_m = \frac{1}{2\sqrt{\gamma l} + \tau} \qquad v_m = \sqrt{\frac{\gamma}{l}} \qquad k_m = \frac{l}{\gamma^2 + +\tau\sqrt{\gamma l} + l^2}$$

Similarly, GDR yields:

$$q_m = \frac{v_f}{\tau v_f + l} \qquad v_m = v_f \qquad k_m = \frac{1}{\tau v_f + l}$$

LCM does not yield a closed form of capacity, but can be solved numerically.

It is interesting to note that, in SDR, capacity is irrelevant to free-flow speed, while both GDR and LCM predict that capacity is a function of free-flow speed. The effect is also illustrated in the top left subplot of Figure 4.

**Effective Vehicle Length**

Effective vehicle length $l_i$ is the the longitudinal space that a driver sees him or herself representing in the traffic. It is typically regarded as the physical vehicle length plus some buffer spaces at both ends. It is also viewed as the bumber-to-bumber spacing when traffic is jammed. When aggregated over vehicles, effective vehcile length is the reciprocal of jam density: $l_i \to l = 1/k_j$. Unlike free-flow speed which is accurately visible in field data, jam density is seldom revealed, see Figures 1 to 3. However, it can be deduced by following the trend of the congested region or determined from a reasonable range, e.g., 100 – 200 veh/km based on an effective vehicle length of 5 – 10 m. The influence of $l$ is illustrated in the top right subplot of Figure 4 where $l$ is varying while others parameters are held constant.

In stop-and-go traffic around jammed condition, the stopping or moving of vheicles propergates backward progressively forming a kinematic wave at jam density $\boldsymbol{\omega_j}$. Since drivers react strickly according to driving rules, the speed of kinematic wave at jam density $\omega_j$ can be determiend as:

SDR: $\omega_j = \left.\frac{dq}{dk}\right|_{k=k_j} = \left(v - \frac{\gamma v^2 + \tau v + l}{2\gamma v + \tau}\right)_{v=0} = -\frac{l}{\tau}$

GDR: $\omega_j = \left.\frac{dq}{dk}\right|_{k=k_j} = -\frac{l}{\tau}$

LCM: $\omega_j = \left.\frac{dq}{dk}\right|_{k=k_j} = -\frac{l}{\tau + l/v_f}$

Apparently, effective vehicle length affects $\omega_j$ and the effect is also illustrated in the top right subplot of Figure 4. Assume effective vehicle length of 6 meters, perception reaction time of 1 second, and free-flow speed of 30 m/s (or 108 km/hr), safe and good driving rules suggest an $\omega_j$ of -21.6 km/hr, LCM results in -18 km/hr. These results are in agreement with field observations as well as literature, e.g., -23 km/hr in Lighthill and Whitham [17] and -20 km/hr in Del Castillo [18].

As discussed above, effective vehicle length also affects capacity condition – its magnitude and location.

**Perception-Reaction Time**

Though free-flow speed appears insensitive to perception-reaction time $\tau_i$, capacity is heavily influenced by this parameter as confirmed by the capacity condition above. Since $\tau_i$ represents how fast a driver responds to stimuli, e.g., braking light of the front vehicle, it mainly takes effect in relatively dense traffic where drivers need to pay attention to surrounding vehicles, especially the leading one. Therefore, the congested region is also heavily influenced by perception-reaction time. A disturbance in traffic is almost sure to be picked up by following vehicles and gets propagated upstream. Hence, backward wave speed $u$ has a close relationship with $\tau_i$. As a boundary condition, the speed of backward wave at jam density $\omega_j$ was given above. In general, the shorter the perception-reaction time (i.e., $\tau_i \downarrow$), the greater the backward wave speed in magnitude (i.e., $|u| \uparrow$), and hence the steeper (more negative) the congested branch of the corresponding flow-density relationship. The effects are illustrated in the bottom left subplot of Figure 4.

As the congested branch becomes steeper, it meets the free-flow branch at higher flow rates suggesting greater capacities. However, it seems that perception-reaction time is not the only parameter that dictates how the two branches meet and hence the underlying flow-density relationship.

**Aggressiveness**

It turns out that aggressiveness $\gamma_i$ plays an even more important role in the shaping of fundamental diagram, more specifically, capacity condition (magnitude and location), the transition around capacity, and whether or not there is capacity drop phenomenon.

In the safe driving rule, aggressiveness assumes positive values $\gamma_i > 0$, which corresponds to "timid" drivers who need extra room for increased safety. As drivers become more "timid" (i.e., $\gamma_i \uparrow$), they will need longer safe distances, and hence less fow can be sustained. This relationship is reflected in the capacity condition given above.

In addition, "timid" traffic (i.e., $\gamma > 0$) results in early termination of free-flow condition and early onset of congested condition because drivers tend to respond to leading vehicles at lower density than that would be for normal (i.e., $\gamma = 0$) or aggressive (i.e., $\gamma < 0$) traffic. Meanwhile, the transition is smooth, i.e., a skewed parabola flow-density curve is resulted around capacity condition. See the bottom right subplot of Figure 4.

The good driving rule does not have an aggressiveness term, which can be viewed as $\gamma_i = 0$. Since aggressiveness is zero here, it does not play a role in the formula of capacity condition. Meanwhile, zero aggressiveness in the good driving rule always yields a triangular flow-density relationship, meaning discontunity is introduced at capacity condtion $(q_m, k_m)$ where the free-flow condition (i.e., $q = v_f k$) and congested condition (i.e., $q = \frac{1}{\tau} - \frac{l}{\tau} k$) meet.

LCM does not pre-assume a value for $\gamma_i$ which can be possitive, zero, or negative depending on driver population. When traffic exhibits aggressive characteristic (i.e., $\gamma < 0$), LCM predicts that free-flow condition may sustain up to very high flow rates (e.g. over 3000 veh/hr) before giving in to congested condition. In addition, such a transition can be a drastic one in that flow drops significantly when the changeover takes place. It appears as though there were two capacities here. One is resulted when loading traffic onto an empty highway. Flow increases linearly with density. As density continues increasing, flow keeps its momentum and rises up to levels that normally require drivers to observe safe distance. At this point, traffic seems to be over-saturated. Consequently, a little disturbance in traffic would result in fast deterioration in condition. All of sudden, traffic becomes packed with a significant drop in speed and flow. Another capacity is typically resulted during an unloading process from congested condition. As traffic keeps recovering toward the free-flow side, no capacity jump is observed around the pervious transition point. Instead, the new transition takes place smoothly as in Figure 3, which suggests another capacity that is lower than the previous one, i.e., a capacity drop phenomenon. This results in a reverse-lambda flow-density relationship that neither of the other two models captures and the effect is illustrated in the bottom right subplot of Figure 4.

The above discussion of influence of human factors parameters is summerized in Table 1.

**TABLE 1 Influence of Human Factors on Fundamental Diagram**

| Human Factor Parameters | $v_i$ | $l_i$ | $\tau_i$ | $\gamma_i$ |
|---|---|---|---|---|
| Free-flow speed $v_f$ | Y | N | N | N |
| Capacity – magnitude $q_m$ | N Y Y | Y | Y | Y N Y |
| Capacity – location $k_m$ | N Y Y | Y | Y | Y N Y |
| Capacity – transition | N N Y | N | N N Y | Y |
| Capacity – drop | N N Y | N | N N Y | N N Y |
| Backward wave speed at jam $\omega_j$ | N | Y | Y | N |
| Jam density $k_j$ | N | Y | N | N |

Note: Y – has influence; N – no influence. Single letter denotes that the same comment applies to the three models. Three letters (e.g., N N Y) means the comments of SDR, GDR, and LCM, respectively.

## WHAT DO EMPIRICAL DATA SAY?

### Loading Processes at a Few Locations

Generated from highway data at a few locations world wide, Figure 5 samples the temporal development of loading processes on these highways including Autobahn in Germany, Amsterdam Ring Road, Highway 401 in Canada, I-4 in Orlando, and PeMs in California.

First of all, it is clear that free-flow condition is rather linear across the board, suggesting that drivers are not sensitive to leading vehicles and are free to choose their desired speeds. Note that

free-flow speeds differ on different highways suggesting that drivers' choice of desired speeds is location-specific.

Remarkable in the figure is when the curves peak as the loading process proceeds. For instance, the free-flow curve of PeMs is only sustainable a little over 1000 veh/hr, while those of Amsterdam and Autobahn maintain up to about 2500 veh/hr. Though unknown without field measurement, perception-reaction time can be roughly deduced from peak flow rates. For example, according to the good driving rule, average headway $h$ is perception-reaction time plus a little buffer, $h = \tau + l/v_f$ , PeMs data suggest a perception-reaction time of a little less than 3.0 seconds, while that of Amsterdam is roughly 1.4 sec. Given that free-flow speed is about the same at the two locations, one would conclude that drivers at the two locations have about the same taste of desired speed but in general take differently time to react to leading vehicles.

Also striking in the figure is how the curves peak. More specifically, this concerns how free-flow condition gives in to congested condition. For example, PeMs and Amsterdam data seem to transition along a "skewed parabola" curve; I-4 data suggest a "triangular" changeover; Autobahn and Highway 401 data appear to experience a capacity drop when the congested region takes over, i.e. a "reverse-lambda" shape.

To the minimum, Figure 4 reveals that different locations give rise to different driver characteristics which, in turn, result in different traffic flow characteristics. For example, the five sets of data suggest different free-flow speeds, different peak flow rates, different peak densities, and different transition curves. This poses a great challenge to traffic flow modeling which should not only capture the underlying mechanism but also the wide ranges of variability.

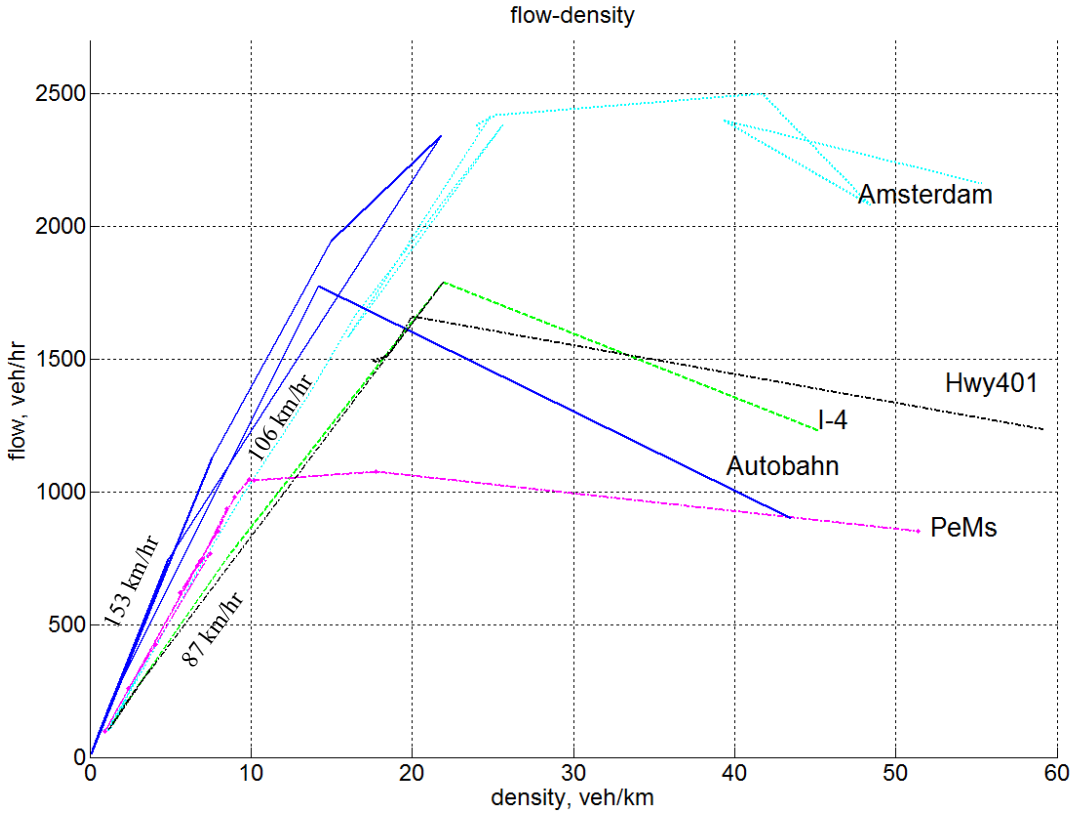


**FIGURE 5 Temporal development of flow-density relationship on selected highways**

## Fitting Models to Empirical Data

As a measure of how close modelling matches field observations, Figure 6 illustrates the result of fitting the three models to GA400 data with fitted parameters tabulated in Table 2.

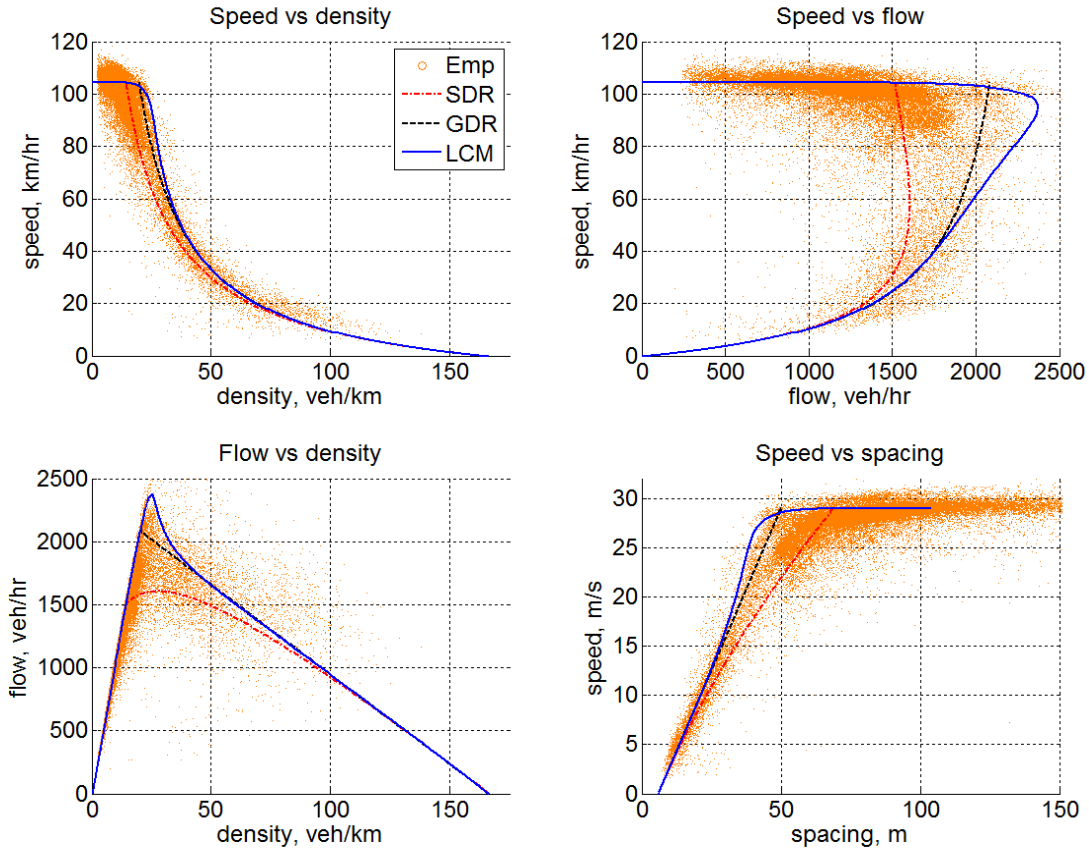


Note: SDR – safe driving rule; GDR – good driving rule; LCM – longitudinal control model

**FIGURE 6 Three models fitted to empirical data**

**TABLE 2 Human factors parameters fitted to empirical data**

| Model | $v_f$ (m/s) | $\tau$ (s) | $l$ (m) | $\gamma$ (s$^2$/m) |
|---|---|---|---|---|
| Safe driving rule | 29 | 1.5 | 6 | 0.023 |
| Good driving rule | 29 | 1.5 | 6 | 0 |
| LCM | 29 | 1.3 | 6 | -0.041 |

The figure shows that the three models perform almost the same when traffic is light and severely congested. However, the difference is salient in the transition from free flow to congestion, particularly around capacity condition.With similar settings except for aggressiveness, the safe driving rule yields the lowest capacity, while LCM suggests the highest and also the closest to true capacity. This result tends to support the significance of aggressiveness in traffic flow modeling.

Perhaps more prominent in the figure is the transition around capacity. The safe driving rule with $\gamma = 0.023$ (meaning "timid" drivers) corresponds to a skewed parabola transition; good driving rule with $\gamma = 0$ (meaning "normal" drivers) introduces discontinuity that yields a triangular

transition; LCM with $\gamma = -0.041$ produces a reverse-lambda transition suggesting a possible capacity drop.

In traffic flow modeling, it is important to faithfully reproduce free-flow, congested, and jammed conditions. Even more important is to capture capacity condition. As evidenced above, aggressiveness plays a differentiating role in capacity condition – magnitude, location, transition, and capacity drop. In addition, it is attractive for a model to represent a spectrum of transition around capacity such as skewed-parabola, triangular, and reverse-lambda since they are all observed in the field. Note that the safe driving rule captures only the first type; good driving rule always yields the second type; LCM is able to represent all three types, see Figure 4.

Though Figure 6 only reveals a likely reverse-lambda transition around capacity and a possible capacity drop, these phenomena are confirmed in Figure 3 with temporal development of loading and unloading processes illustrated. Combined, Figures 3 and 6 seem to alert us to the possibility that loading and unloading processes may follow different speed-density relationships. For example, the loading process may be a reverse-lambda type, while the unloading is a skewed parabola or a triangle. If this is true, then two issues naturally follow. First, this observation seems to suggest that driver characteristics may be different during loading and unloading processes, and perhaps they may even be dynamic within a driving process. Such an effect is typically not captured in conventional modelling approaches. For example, perception-reaction time is normally treated as a constant in our models unless a stochastic approach is taken. Second, this observation may imply different types flow-density relationship for the same traffic during different processes. This requires that the underlying model be flexible enough to capture all of them without having to resort to another model. LCM is an example in case. Similarly, Chamberlayne et al [5] produced the effect of capacity drop in INTEGRATION by varying vehicle acceleration behavior without having to introducing a discontinuous flow-density relationship.

## ESTIMATION OF HUMAN FACTORS PARAMETERS

Involving measuring parameters, model calibration can be a time- and resource- consuming task, especially when sampling and aggregating a large population becomes necessary. This section intends to supplement such an endeavor with a quick, rough estimate by only examining traffic flow data which are readily available in most Intelligent Transportation Systems (ITS).

Assume one starts with an empirical diagram such as the “clouds” in Figures 1, 2, and 6 and somehow a flow-density relationship is sketched, as curve 1 in Figure 7. Since field data typically show clear trend of free-flow condition, free-flow speed $v_f$ can be found easily as the slope of the trend line in free-flow region. In addition, field data may also reveal a trend of congested condition. Following the trend, one may find jam density $k_j$ as the intersection of the trend line and the horizontal axis.

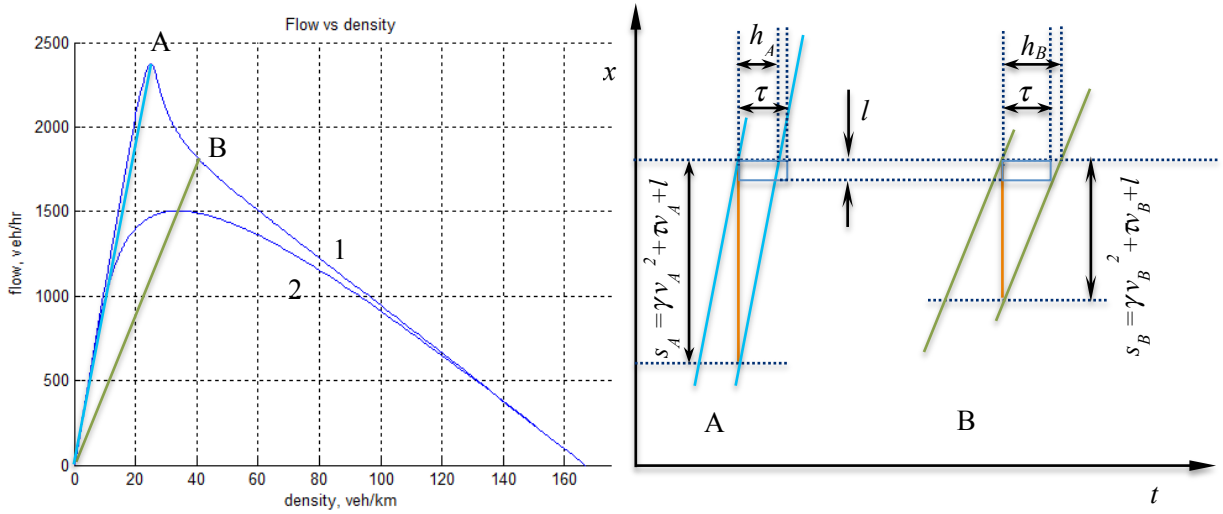


**FIGURE 7 Estimation of human factors parameters**

Estimation of the remaining two human factors parameters, namely perception-reaction time $\tau$ and aggressiveness $\gamma$, necessitates two known points A and B on the curve. Though in the figure A appears to be the capacity and B possibly the reduced capacity, they don't have to be special in order to apply the estimation method. Since conditions at A$(q_A, k_A, v_A)$ and B$(q_B, k_B, v_B)$ are known, their average microscopic characteristics A$(h_A, s_A, v_A)$ and B$(h_B, s_B, v_B)$ can be calculated. Sketched on the right of Figure are trajectories of imaginary vehicles operating at conditions A and B. Using geometry of the trajectories and car-following rules, the following can be established:

$$\begin{cases} s_A = \gamma v_A^2 + \tau v_A + l \\ s_B = \gamma v_B^2 + \tau v_B + l \end{cases}$$

Solving the above system of equations yields the following estimates:

$$\begin{cases} \gamma = \dfrac{(s_A v_B - s_B v_A) - l(v_B - v_A)}{v_A^2 v_B - v_A v_B^2} \\ \tau = \dfrac{-(s_A v_B^2 - s_B v_A^2) + l(v_B^2 - v_A^2)}{v_A^2 v_B - v_A v_B^2} \end{cases}$$

Unlike what is required by the safe driving rule, the figure purposely shows that the headway of condition A, $h_A$, is shorter than perception reaction time. This is to alter readers to the possibility that aggressive drivers may follow the leader closer than that stipulated by the good driving rule, i.e., $\gamma < 0$. Paradoxically, short headways are frequently observed in traffic particularly in inner lanes, but car-following accidents are few. Harris [14] was probably right that this is so "not because the separations which drivers allow are necessarily safe but because the emergencies that reveal the danger are rare".

## CONCLUSIONS

This research examined the role of human factors such as aggressiveness, perception-reaction time, desired speed, and effective vehicle length in microscopic car following and traced their way into macroscopic traffic flow representation, i.e., fundamental diagram. Then, the influence of these human factors on the diagram was analyzed with reference to empirical observations in the field.

The findings of this research are summarized as follows. First, all four factors are actively involved in characterizing traffic flow, though they play different roles in fundamental diagram. More specifically, desired speed affects free-flow speed which, in turn, dictates free-flow condition. Effective length dictates jam density and affects backward wave speed at jam density. Perception-reaction time plays a significant role in virtually all aspects of fundamental diagram. In particular, perception-reaction time is critical in determining capacity (magnitude and location). No less than that of perception-reaction time, the role of aggressiveness has long been overlooked. Contrary to what is commonly believed, empirical evidences show that drivers will follow at distances shorter than what is deemed as safe. Hence, aggressiveness is related to a driver's willingness to tailgate in pursuit of speed gain. This research reveals that aggressiveness is the key to unlock the mysteries in fundamental diagram such as reverse-lambda flow density relationship and capacity drop.

In addition, empirical observations seem to suggest that driver characteristics may be different during loading and unloading processes, and perhaps they may even be dynamic within a driving process. Such an effect is typically not captured in conventional modelling approaches. For example, perception-reaction time is normally treated as a constant in our models unless a stochastic approach is taken. Meanwhile, empirical observations may imply different types flow-density relationship for the same traffic during different processes. This requires that the underlying model be flexible enough to capture all of them without having to resort to another model.

Moreover, this research provides a quick estimation method to roughly deduce human factors parameters from macroscopic traffic flow data without resorting to microscopic vehicle trajectory data. However, this estimation method is intended as a supplement rather than a replacement to field measurements.

## ACKNOWLEDGEMENT

This research is partly supported by University Transportation Center (UTC) program.

## REFERENCES

[1] M. Koshi, M. Iwasaki, and I Okhura, "Some findings and an overview on vehicular flow characteristics," in *The 8th International Symposium on Transportation and Traffic Flow Theory (Edited by Hurdle, V.F., Hauer, E. and Steuart, G.F.)*, University of Toronto Press, Toronto, Canada, 1983, pp. 403-426.

[2] J. H. Banks, "Freeway speed-flow-concentration relationships: more evidence and interpretations," *Transportation Research Record*, vol. 1225, pp. 53-60, 1989.

[3] J.H. Banks, "Review of Empirical Research on Congested Freeway Flow," *Transportation Research Record*, vol. 1802, pp. 225–232, 2002.

[4] Meead Saberi and Hani Mahmassan, "Capacity Drop Phenomena in Urban Networks," in *Midyear Meetings and Symposium on Innovations in Traffic Flow Theory*, Fort Lauderdale, FL, USA, 2012.

[5] Chamberlayne E., Rakha H., and Bish D, "Modeling the Capacity Drop Phenomenon at Freeway Bottlenecks using the INTEGRATION Software," *Transportation Letters: The International Journal of Transportation Research*, vol. 4, no. 4, pp. 227-242, 2012.

[6] AASHTO, *A Policy on Geometric Design of Highways and Streets, 6th Edition*.: the American Association of State Highway and Transportation Officials, 2011.

[7] Roger P. Roess, Elena S. Prassas, and William R. McShane, *Traffic Engineering, 4th Edition*.: Prentice Hall, 2010.

[8] Walter P. Kilareski, Scott S. Washburn Fred L. Mannering, *Principles of Highway and Traffic Engineering*, 5th ed.: John Wiley & Sons, 2012.

[9] T. Forbes and M. Simpson, "Driver and Vehicle Response in Freeway Deceleration Waves," *Transportation Science*, vol. 2, no. 1, pp. 77-104, 1968.

[10] L. A. Pipes, *Journal of Applied Physics*, vol. 24, pp. 271-281, 1953.

[11] P. Gipps, "A Behavioral Car Following Model for Computer Simulation," *Transportation Research, Part B*, vol. 15, pp. 105-111, 1981.

[12] TRB, *Highway Capacity Manual*.: U.S. Government Printing Office, Washington DC., 1950.

[13] TRB, *Revised Traffic Flow Theory Monograph*.: Transportation Research Board. Washington DC., 2001.

[14] Harris, "Following Distances, Braking Capacity and the Probability of Danger of Collision Between Vehicles," *Austrian Road Research Board, Proceedings 2, Part 1*, pp. 496-512.

[15] Daiheng Ni, "A Unified Perspective on Traffic Flow Theory, Part I: The Field Theory," *Applied Mathematical Sciences*, vol. 7, no. 39, pp. 1929-1946, 2013.

[16] T. Forbes, *Highway Research Record*, vol. 15, pp. 60-66, 1963.

[17] Lighthill M. J. and Whitham G. B., "On Kinematic Waves: a Theory of Traffic Flow on Long Crowded Roads," *Proc. of the Royal Society, Series A*, vol. 229, pp. 317-345, 1955.

[18] Del Castillo and F.G. Benítez, "On the functional form of the speed-density relationship—I: General theory," *Transportation Research Part B: Methodological*, vol. 29, no. 5, pp. 373–389, 1995.